Infrared Signatures of a Water Molecule Attached to Triatomic Domains of Molecular Anions: Evolution of the H-bonding Configuration with Domain Length

William H. Robertson, Erica A. Price, J. Mathias Weber, Joong-Won Shin, Gary H. Weddle, and Mark A. Johnson*

Sterling Chemistry Laboratory, Yale University, P.O. Box 208107, New Haven, Connecticut 06520

Received: April 17, 2003; In Final Form: June 17, 2003

We present mid-IR argon predissociation spectra for a series of complexes, $M^-\cdot H_2O$ ($M = CS_2^-$, OCS^-, SO_2^-, $CH_3NO_2^-$, $CH_3CO_2^-$, and NO_2^-), chosen to explore how changes in the triatomic binding site affect the H-bonding configuration of the attached water molecule. With the exception of NO_2^-, the calculated global minima on the potential surfaces of all of the complexes occur in a configuration where both OH groups are attached to the anion. The observed spectra, on the other hand, fall into three distinct categories. Simple spectra characteristic of the double ionic H-bonding arrangement are observed for the monohydrates of SO_2^-, OCS^-, and CS_2^-, whereas the $CH_3NO_2^-\cdot H_2O$ and $CH_3CO_2^-\cdot H_2O$ spectra are complicated, displaying a progression of closely spaced bands with a broad, bell-shaped envelope beginning several hundred wavenumbers below the calculated fundamentals. Although the spectrum of the $NO_2^-\cdot H_2O$ complex is the most red-shifted, it is again simple, reflecting the expected asymmetric (single ionic H-bonded) motif. These data indicate that the transition from single to double ionic H-bonding occurs at a critical domain length of about 2.2 Å. We explore the potential surfaces governing the interconversion between the two forms with density functional calculations and construct vibrationally adiabatic potential surfaces to assess the cause of the spectral complexity displayed by the methylated anion hydrates.

I. Introduction

When a water molecule binds to small anions such as the monatomic halides, X^-, the isolated $X^-\cdot H_2O$ complexes generally adopt the asymmetric, single ionic H-bonded (SIHB) motif[1−3] found in the first hydration shell surrounding these ions in aqueous solution.[4] The SIHB structure is immediately evident in the mid-IR spectrum, where the OH bound to the ion oscillates hundreds of wavenumbers below the free OH group, which appears very close to the centroid of the bands in isolated H_2O (3707 cm^{-1}). For larger systems, such as the Cu^- anion[5] and molecular anions with especially extended charge distributions,[6,7] however, the symmetrical form is calculated to be favored, where the water molecule binds along the symmetry axis in a double ionic H-bonding (DIHB) configuration. This symmetrical structure has recently been observed experimentally[8] in the $SO_2^-\cdot H_2O$ complex through its vibrational spectrum in the OH stretching region, which is dominated by a single, sharp band assigned to the symmetric stretching vibration. In this report, we follow the evolution of the OH stretching spectra displayed by a water molecule bound to a variety of triatomic anions as well as to more complex organic anions which feature a triatomic binding site. Specifically, we contrast the behavior of the CS_2^-, OCS^-, SO_2^-, $CH_3NO_2^-$, $CH_3CO_2^-$, and NO_2^- ions, a series which explores how properties of the ions, such as the physical separation of the H-bonding centers and their proton affinities, affect the morphologies of the monohydrates. With the exception of the $NO_2^-\cdot H_2O$ complex, all of these species are calculated to adopt the DIHB motif in their minimum energy structures.

It seems reasonable to imagine that there is a continuous evolution between the SIHB and DIHB forms of the anion monohydrates, and the critical factor governing the observed geometry is the magnitude of the barrier in the (double minimum) water-rocking potential which characterizes the SIHB configuration. The large difference in OH stretching frequencies between the strongly red-shifted SIHB[1,9,10] and weakly red-shifted DIHB[8] forms further introduces the possibility of an unusually strong interaction between the OH stretching motions and the soft modes which mediate interconversion between these isomeric configurations. We explore the magnitude of this coupling using a vibrationally adiabatic approach and point out that effective potential curves governing the rocking motion of the water molecule (i.e., those which preserve the excitation in the OH stretching degree of freedom) are likely to have very different shapes depending on the extent of OH excitation. An analogous scenario has been observed previously in the C_3 molecule,[11] where the ground state is linear, but the vibrational states involving excitation of the asymmetric stretching vibration are bent.

II. Experimental Section

Vibrational spectra in the OH stretching region were obtained by argon predissociation spectroscopy:[12]

$$M^-\cdot H_2O\cdot Ar_n + h\nu \rightarrow M^-\cdot H_2O\cdot Ar_{n-m} + m\mathrm{Ar} \qquad (1)$$

The argon predissociation method has two distinct advantages over experiments on the bare complexes. First, the argon "tagged" clusters allow mass spectrometric isolation of the coldest clusters ($E_{int} \sim D_0(M^-\cdot Ar)$)[13] formed in the ion source, and second, the argon atoms provide weakly bound "messengers"[14,15] which enable mid-IR absorption spectra of strongly bound cluster ions to be recorded by vibrational predissociation.

* To whom correspondence should be addressed.

10.1021/jp030474v CCC: $25.00
Published on Web 08/06/2003

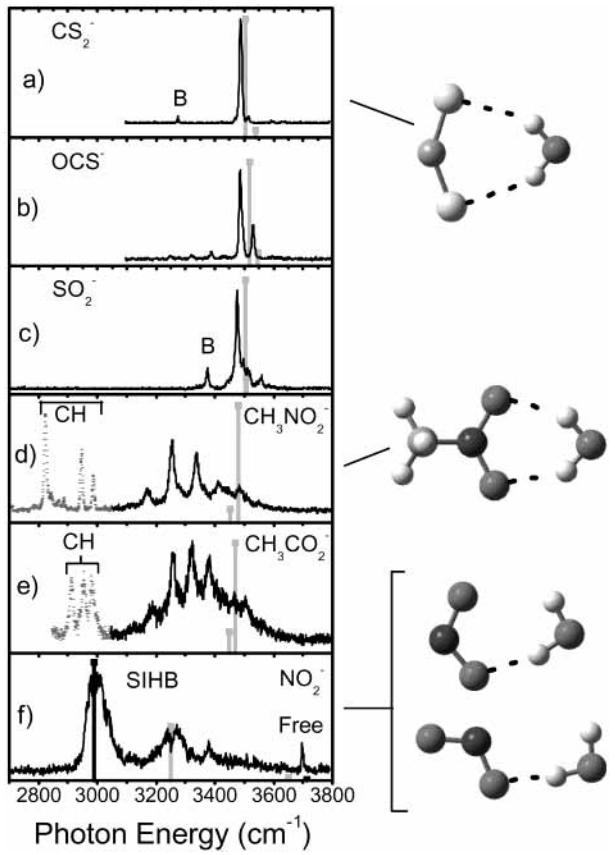

Figure 1. Mid-IR argon predissociation spectra of the anion monohydrates: (a) $CS_2^-\cdot H_2O\cdot Ar_4$, (b) $OCS^-\cdot H_2O\cdot Ar$, (c) $SO_2^-\cdot H_2O\cdot Ar_3$ (taken from ref 8), (d) $CH_3NO_2^-\cdot H_2O\cdot Ar$, (e) $CH_3CO_2^-\cdot H_2O\cdot Ar$, and (f) $NO_2^-\cdot H_2O\cdot Ar_5$. B = water intramolecular bending overtone, (CH) = anion CH stretch fundamentals, (SIHB) = single ionic H-bond OH stretch fundamental, and (Free) = free OH stretch fundamental. The inset structures of $CS_2^-\cdot H_2O$ (upper), $CH_3NO_2^-\cdot H_2O$ (middle), and two forms of the $NO_2^-\cdot H_2O$ complex (lower) were optimized at the B3LYP/aug-cc-pVDZ level. The vertical bars denote calculated frequencies, scaled by 0.9627 to approximately correct for anharmonicity at this level of theory. The gray bars denote calculated anharmonic frequencies for front-side geometries, whereas black bars indicate the frequencies associated with the backside geometry found to occur in $NO_2^-\cdot H_2O$.

Spectra were obtained with different numbers of argon atoms attached in order to establish the dependence of the observed band patterns on the extent of argon solvation.[16−18]

The argon-solvated anion clusters were formed in a pulsed supersonic entrainment reactor[19] where the neutral precursor of the desired anion and water vapor are independently introduced on the low pressure side of an electron beam-ionized expansion containing only argon. Mass selection was achieved using the Yale tandem time-of-flight photofragmentation spectrometer described previously,[20] which utilizes an ion bunching strategy to match the ion source duty cycle with that of broadly tunable pulsed lasers. Tunable mid-IR radiation was generated in a KTP/KTA optical parametric oscillator/amplifier (Laser Vision). The spectra are normalized for laser energy fluctuations over the scan and result from the summation of typically 10−20 individual scans.

Geometry optimizations and harmonic frequency calculations were performed at the B3LYP/aug-cc-pVDZ level as implemented in the Gaussian 98 package.[21]

III. Results and Discussion

IIIa. Appearance of the Spectra. Figure 1 presents mid-IR argon predissociation spectra of a series of monohydrates involving molecular anions with triatomic binding sites. The spectra are arranged from top to bottom in order of decreasing binding site length (i.e., the distance between the terminal atoms, recorded in Table 1) with CS_2^- the longest and NO_2^- the shortest. The OH stretching spectra of the monohydrates with the sulfur-containing anions (having the longest binding sites) are simplest and are similar to each other, with the observed band positions collected in Table 2. Each spectrum displays a sharp dominant band near 3500 cm^{-1} with a conspicuous absence of absorption in the vicinity of the free OH stretch near 3700 cm^{-1}. This is the spectroscopic signature of DIHB binding recently discussed[8] in detail in the $SO_2^-\cdot H_2O$ case, which was analyzed with the aid of an isotopic substitution study and ab initio calculations. We therefore assign the dominant band in sulfur-containing ions (Figure 1a−c) to the symmetric stretching fundamental (ν_1). Definitive assignments of the weaker asymmetric stretching (ν_3) fundamentals, expected to occur just above the ν_1 origin in the sulfur species, are complicated by the presence of combination bands involving the ion−molecule soft modes in this region. The weaker bands below the dominant symmetric stretch fundamental in Figure 1a−c are likely due to the overtone of the HOH intramolecular bending vibration (B), which usually appears via a Fermi-type mixing with the stretching mode.[1,22] The fact that several such bands occur in the $OCS^-\cdot H_2O$ spectrum (Figure 1b) probably reflects a strong mixing of the water intramolecular bend and energetically nearby CO stretch fundamentals, such that overtones of these mixed levels interact with the symmetric OH stretch. Note that alternative, covalently bound forms of these ions (for example, the anion of the H_2SO_3 acid) are calculated to display much more red-shifted OH stretching fundamentals and, consequently, are not likely to be the carriers of the observed bands.

The complexes with methylated anions, $CH_3NO_2^-\cdot H_2O$ and $CH_3CO_2^-\cdot H_2O$, are also calculated to adopt symmetrical DIHB structures and therefore would be expected to display spectra similar to the hydrates of the sulfur-containing anions (calculated frequencies indicated by gray bars in Figure 1, parts d and e). Surprisingly, the observed spectra consist of extended OH band progressions beginning several hundred wavenumbers below the calculated stretching energies, ruling out an assignment scheme

TABLE 1: Geometrical Parameters Calculated at the B3LYP/aug-cc-pVDZ Level

complex	distance (Å)		X···H−O angle (deg)	H−O−H angle (deg)
$CS_2^-\cdot H_2O$	S−S	3.13	148	100.5
$OCS^-\cdot H_2O$[a]	O−S	2.72	150, 140	99.6
$SO_2^-\cdot H_2O$[b]	O−O	2.62	147	97.8
$CH_3NO_2^-\cdot H_2O$	O−O	2.30	145	95.5
$CH_3CO_2^-\cdot H_2O$	O−O	2.27	144	95.9
$NO_2^-\cdot H_2O$[c]	O−O	2.15	165, 119	97.6

[a] Reference 7 reports 2.707 Å, 146.6°, and 99.1° at the CCSD/6-311++G(d,p) level. [b] Reference 8 reports 2.633 Å, 148.6°, and 96.7°at the MP2/aug-cc-pVDZ level. [c] Front side isomer (upper structure in Figure 1f).

TABLE 2: Experimental Vibrational Bands (cm^{-1}) of Triatomic Anion Monohydrates (±5 cm^{-1})

	symmetric OH stretch	bending overtone
$CS_2^-\cdot H_2O$	3488	3275
$OCS^-\cdot H_2O$	3486	3388, 3322, 3248[a]
$SO_2^-\cdot H_2O$[b]	3475	3376
$NO_2^-\cdot H_2O$	2995[c]	

[a] See text for discussion of these assignments. [b] Taken from ref 8. [c] Single ionic H-bonded OH stretch fundamental in this asymmetric complex.

TABLE 3: Experimental CH Stretching Frequencies of Parent Neutral, Bare, and Monohydrated Organic Anions

	A′ CH_3 symmetric stretch	A′ CH_3 asymmetric stretch	A" CH_3 asymmetric stretch	OH stretch
CH_3NO_2[a]	2974	3045	3080	
$CH_3NO_2^-$[b]	2777	2924	2967	
$CH_3NO_2^-\cdot H_2O$	2823	2947	2986	3170, 3255, 3337, 3412, 3483, 3550
CH_3COOH[c]	2961	2997	3048	
$CH_3CO_2^-$	2902	2941, 2953[d]	2967	
$CH_3CO_2^-\cdot H_2O$	2912	2953	2980	3188, 3258, 3321, 3381, 3506

[a] Taken from ref 34. [b] Taken from ref 23. [c] Taken from ref 35. [d] The doubling of this band is likely due to interaction with a CH_3 deformation mode, as is known to complicate the methyl vibrations of other small molecules.[36]

based on OH stretch fundamentals. We will discuss likely causes for this behavior at length in section IIIe. The sharp bands in the 2800−3000 cm^{-1} region (shaded gray in Figure 1, parts d and e) are due to excitations of the methyl group CH stretching modes. The CH stretching bands are compared with those of the bare anions and corresponding neutral species in Table 3. Note the large (100−200 cm^{-1}) red-shifts of the CH stretches in the $CH_3NO_2^-$ ion[23] relative to those in the bare neutral. This arises[23] from the bent $-NO_2$ group, which accommodates the excess electron in the HOMO largely localized on the nitrogen atom. Interestingly, the red-shifts are significantly reduced (recovering about one-fourth of the displacement observed upon formation of the bare anion) when a water molecule is attached to $CH_3NO_2^-$. Apparently, the charge redistribution upon hydration causes a shift in electron density toward the water molecule, with a concomitant relaxation of the anion structure closer to the neutral geometry.

The $NO_2^-\cdot H_2O$ complex, with the shortest distance between terminal atoms, is calculated to occur in two low-lying isomeric forms, with the structures indicated beside the spectrum (Figure 1f). Both isomers correspond to asymmetric SIHB motifs. The front-side isomer, with a hydrogen oriented toward the oxygen atom of NO_2^-, is calculated to display a somewhat red-shifted "free OH" feature (3652 cm^{-1}), whereas the backside isomer is calculated to lie about 300 cm^{-1} lower in energy and should be evidenced by a more typical free OH band (3713 cm^{-1}). The observed, strongly red-shifted OH stretch and, more importantly, the weak free OH feature at 3696 cm^{-1} indeed confirm the formation of an asymmetric (SIHB) complex,[1−3,10] with the strongest features most consistent with the backside hydration motif. The weaker bands near 3250 cm^{-1} could signal the presence of a second, front-side isomer, but could also arise from ion−molecule stretching bands mixed with the intramolecular water bending overtone in this region.

IIIb. Systematics of the OH_{IHB} Shift for the $NO_2^-\cdot H_2O$ Complex. The observation of a triatomic hydrate with an SIHB motif affords the opportunity to compare its spectral behavior with the trends established for SIHB complexes involving monatomic[1,2] and diatomic[9,10] anions. Specifically, we have reported a strong correlation between the OH_{IHB} red-shift and the proton affinity (PA) of the anion,[10] and in Figure 2, we compare the red-shift in the OH_{IHB} fundamental observed in the $NO_2^-\cdot H_2O$ complex with those found in several other systems. The fact that the shift displayed by $NO_2^-\cdot H_2O$ falls quantitatively in line with this trend emphasizes the importance of the chemical (i.e., intramolecular proton-transfer or, equivalently, charge-transfer)[24] interactions in determining the shape of the potential governing the motion of the shared proton. It is noteworthy that the band positions in the DIHB complexes do not follow this trend; for example, the observed transitions for $OCS^-\cdot H_2O$ and $SO_2^-\cdot H_2O$ (filled gray circles in Figure 2) fall about 200 cm^{-1} above the locations of SIHB complexes with similar PA values.[7,25−32]

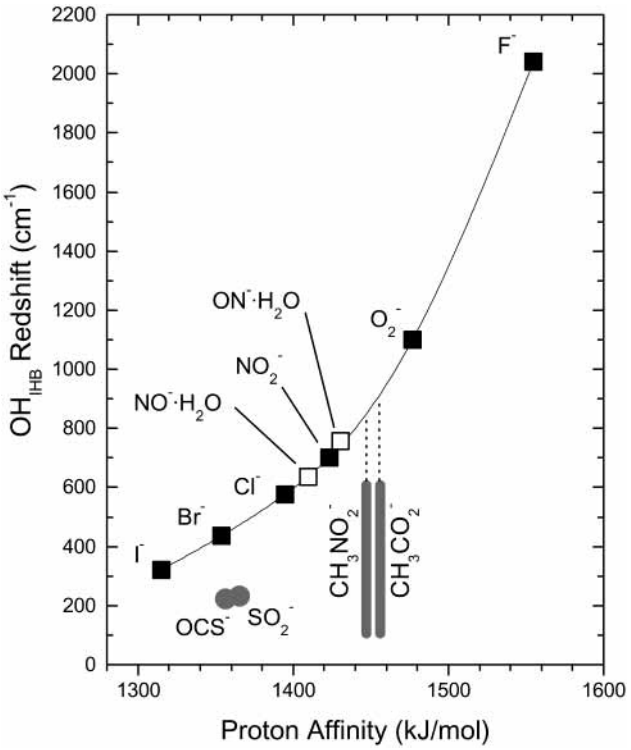

Figure 2. Red-shift of single ionic H-bonded (SIHB) OH stretching fundamentals observed in anion monohydrates[1,2,9,10,16,37,38] as a function of anion proton affinity (PA) (squares).[31] The red-shift vs estimated PA values[7,25−32] of anions that form double H-bonded (DIHB) monohydrates are shown by gray circles and bars, where the length of the bar indicates the energy range of the observed bands. Note that the open squares (□) denote PA values corrected for the energy of the spin-conserving (in this case triplet) proton-transfer products.[10]

IIIc. Barrier Heights and the Evolution from the Double to Single H-Bonding Motif. To explore the mechanics behind the propensity of the larger, sulfur-containing ions to bind a water molecule in the DIHB motif, we first focus on the intramolecular distortion of the water molecule along the H−O−H bending coordinate. Values of the bending angle were extracted from the calculated minimum energy geometries of the complexes and are collected in Table 1. As the distance between terminal atoms in the binding site is reduced, the bending angle of the water molecule reaches a minimum value of about 95.5° in the $CH_3NO_2^-\cdot H_2O$ complex. Further reduction of the distance by 0.15 Å in the NO_2^- ion results in an opening of the monohydrate into a (front-side) SIHB motif, where the release of one of the hydrogen atoms from the ion is accompanied by an increase in the bending angle to 97.6°. In effect, the energetic advantage of forming two H bonds is offset by the distortion imposed on the intramolecular bending coordinate as the binding sites become closer together. It appears that the 2.15 Å separation between oxygen atoms in the NO_2^- anion falls just below the critical length necessary to sustain the DIHB motif.

The key issue concerning the evolution of the binding motif is the height of the barrier separating the two minima in the SIHB geometry. To elucidate the topology of the potential

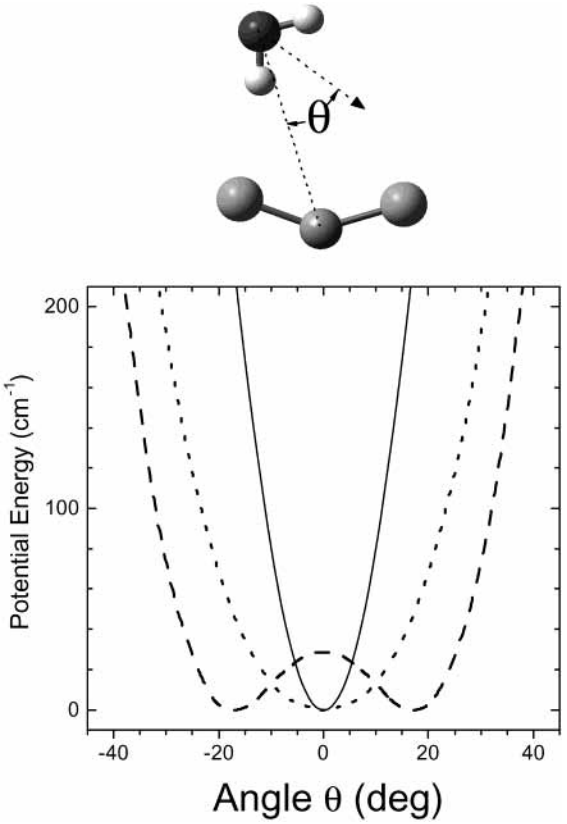

Figure 3. Potential surfaces (calculated at the B3LYP/aug-cc-pVDZ level) as a function of water rocking angle, θ (defined in the upper inset), for the complexes $CS_2^-\cdot H_2O$ (solid), $CH_3CO_2^-\cdot H_2O$ (dotted), and $NO_2^-\cdot H_2O$ (dashed).

surface along the water rocking motion, which mediates interconversion between SIHB and DIHB forms, calculations were carried out on several of the $M^-\cdot H_2O$ systems to determine the rocking angle dependence of the Born−Oppenheimer potential, $U_{BO}(\theta)$. This was accomplished by rotating the water H−O−H angle bisector away from the center atom of the triatomic domain while allowing all other geometrical parameters to relax. Slices of the potential surface along this coordinate are displayed in Figure 3 for the $CS_2^-\cdot H_2O$, $CH_3CO_2^-\cdot H_2O$, and $NO_2^-\cdot H_2O$ (front-side) systems. The CS_2^- and NO_2^- anions were chosen because they display simple examples of DIHB and SIHB binding for comparison with the more complex situation found in the acetate monohydrate. It is clear that, although the potential well is very confined in $CS_2^-\cdot H_2O$, it is quite flat for acetate complex, and a small barrier emerges in the $NO_2^-\cdot H_2O$ system.

IIId. H/D Isotope Study of the $CH_3NO_2^-\cdot H_2O$ Spectra. The surprisingly complex behavior displayed by the methylated anions warrants further consideration. To help clarify the situation, we have acquired the spectra of the $CH_3NO_2^-\cdot HDO$ and $CH_3NO_2^-\cdot D_2O$ complexes in the OD stretching region with the results displayed in Figure 4, again along with the calculated bands expected for the symmetrical complex. These spectra are clearly much simpler than those observed in the OH stretching region, with the dominant bands only about 60 cm^{-1} below the calculated positions. Note the absence of absorption in the vicinity of the free OD stretch (2727 cm^{-1}), again ruling out an SIHB form. Interestingly, both the HDO and D_2O complexes yield remarkably similar patterns consisting of two bands displaced about 87 cm^{-1}, similar to the band spacing of 86 cm^{-1} characterizing the progression in the OH stretching region (Figure 1d). This eliminates assignment of the two bands to

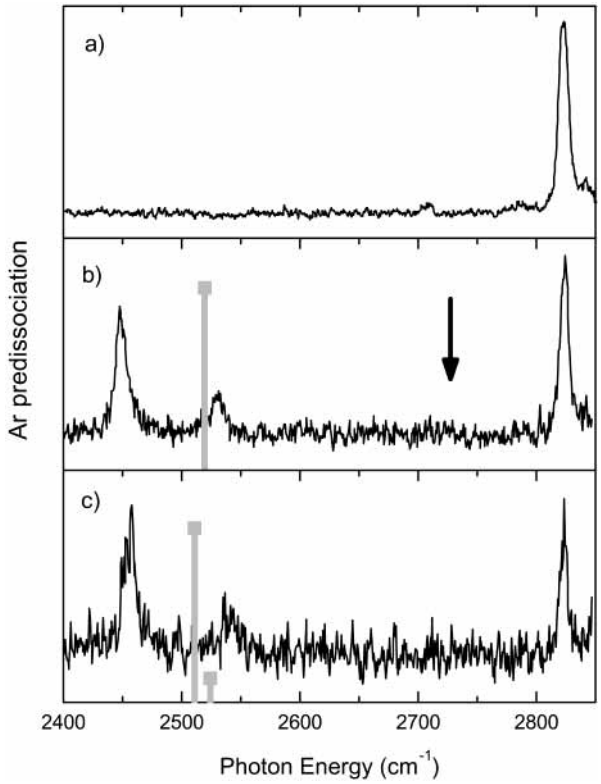

Figure 4. Mid-IR predissociation spectra in the OD region for isotopically substituted $CH_3NO_2^-\cdot H_2O$ complexes: (a) $CH_3NO_2^-\cdot H_2O\cdot Ar$, (b) $CH_3NO_2^-\cdot HDO\cdot Ar$, and (c) $CH_3NO_2^-\cdot D_2O\cdot Ar$. B3LYP/aug-cc-pVDZ calculated frequencies (scaled by 0.9627) are included as gray vertical bars. The arrow indicates the location of the free OD stretching band in isolated HDO.

the ν_1 and ν_3 fundamentals in the $CH_3NO_2^-\cdot D_2O$ complex, and instead favors a scheme where the dominant band is attributed to the symmetric stretch and the band to higher energy assigned as a combination band involving an 87 cm^{-1} soft mode.

IIIe. Remarks on the Origin of the Complexity of the OH Stretching Region in $CH_3CO_2^-\cdot H_2O$ and $CH_3NO_2^-\cdot H_2O$. The isotopic substitution study of the $CH_3NO_2^-\cdot H_2O$ complex described above reveals that, unlike our previous work on the $SO_2^-\cdot H_2O$ complex, the OD and OH regions display very different spectral patterns. This could conceivably be due to mixing with the modes on the anion in the higher energy region, possibly involving the CH stretch levels, and this suggestion can be tested by extending the isotopic study to include $CD_3NO_2^-$. There are other unique aspects of the methylated complexes which deserve consideration, however, in light of the fact that these complexes were calculated to display very flat potential surfaces for the water rocking motion (Figure 3). In the OH stretching region, the maxima in the intensity profiles occur between the modest OH red-shifts observed for the DIHB hydrates and the strong red-shift found in the $NO_2^-\cdot H_2O$ complex. This raises the issue of where the OH_{IHB} transitions *would* occur if the $CH_3CO_2^-\cdot H_2O$ and $CH_3NO_2^-\cdot H_2O$ complexes explore an asymmetric, SIHB configuration in the zero-point motion of a flat surface. A convenient way to display the angle-dependence of the OH stretching frequencies is to construct vibrationally adiabatic potential curves. In fact, such curves have already been invoked to explain the selective excitation of the ion−molecule stretching vibration in combination with the OH_{IHB} fundamental in the SIHB complexes.[1,18] In those cases, the surfaces corresponding to the OH_{IHB} vibrationally excited state are more strongly bound to the ion than those in the ground state,[33] and this displacement in the potential

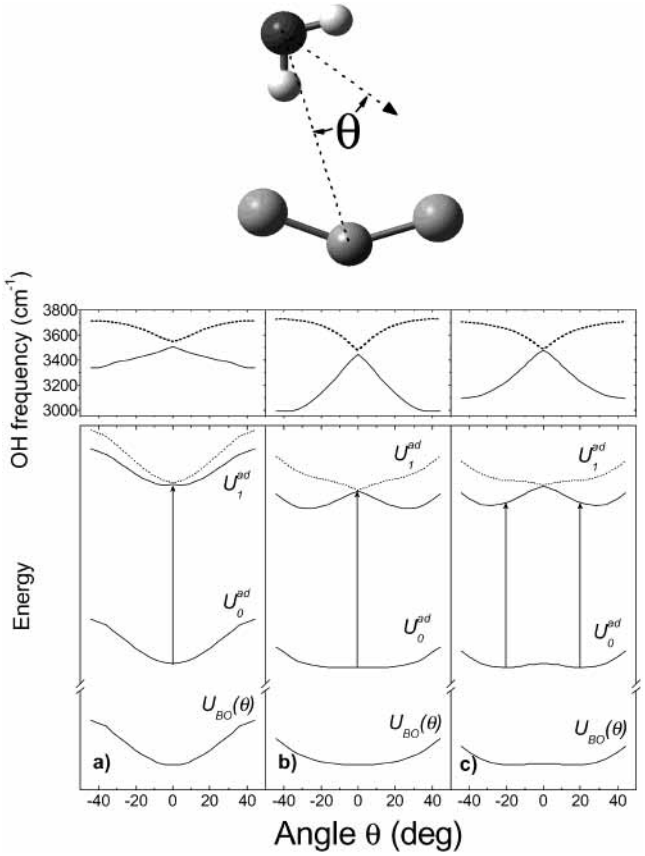

Figure 5. Calculated (B3LYP/aug-cc-pVDZ level) OH stretching fundamentals and water rocking potential surfaces as a function of water rocking angle, θ (defined in the upper inset), for the complexes (a) $CS_2^-\cdot H_2O$, (b) $CH_3CO_2^-\cdot H_2O$, and (c) $NO_2^-\cdot H_2O$. The upper panels present the frequencies of the two OH stretching modes at each rocking displacement, with solid and dashed lines indicating the symmetric and asymmetric stretches, respectively. Note that the symmetric stretch strongly red-shifts at large angle as it evolves into the localized OH_{IHB} stretch. In the lower panels, the bottom trace displays the Born−Oppenheimer potential curve, $U_{BO}(\theta)$, whereas the other traces are vibrationally adiabatic curves generated from eq 2 using $n_i = 0$, $n_j = 0$ for the trace labeled U_0^{ad} and $n_i = 1$, $n_j = 0$ for those labeled U_1^{ad}. The solid and dashed U_1^{ad} curves correlate to excitation of the ionic H-bonded (symmetric) and free (asymmetric) OH stretching motions, respectively.

curves leads to a Franck−Condon-like mechanism for excitation of this soft mode.[18]

The vibrationally adiabatic curves describing effective potentials for the water rocking motion can be constructed from the same calculations used to obtain the potential surfaces displayed in Figure 3. To accomplish this, in addition to the Born−Oppenheimer potential, $U_{BO}(\theta)$, the two harmonic frequencies of the OH stretching modes, $\nu_i(\theta)$, were also recorded at each angle (Figure 5, upper panels). The vibrationally adiabatic potentials, $U_v^{ad}(\theta)$ were then generated according to

$$U_v^{ad}(\theta) = U_{BO}(\theta) + (n_1 + (1/2))h\nu_1(\theta) + (n_2 + (1/2))h\nu_2(\theta) \quad (2)$$

and are dependent on the excitation in each OH stretch mode through the integers n_1 and n_2, with $n_1 = n_2 = 0$ establishing the perturbed shape of the ground-state potential due to the zero-point energies of the OH stretches. The two vibrations, ν_i, correlate to symmetric and asymmetric stretches at the DIHB configuration and to OH_{IHB} and free OH stretches in the SIHB arrangement. The angle-dependence of the two OH stretches is included in the upper panels of Figure 5, and although the frequency changes are large in each case, the effect is most pronounced in the acetate hydrate shown in the center. In fact, the variation of the OH_{IHB} stretch is about 500 cm^{-1} over the range from 0 to 40°.

The resulting BO and vibrationally adiabatic curves (obtained using eq 2 together with the calculated OH stretching frequencies) are compared in the lower panels of Figure 5. The left panel corresponds to the symmetrical $CS_2^-\cdot H_2O$ case and the right panel corresponds to the asymmetrical $NO_2^-\cdot H_2O$ complex. In both of these limiting cases, the general topology of the BO surface survives upon OH vibrational excitation. In fact, the small barrier (28.5 cm^{-1}) on the $NO_2^-\cdot H_2O$ BO surface increases to 52.3 cm^{-1} with the adiabatic correction, which is sufficiently large that the zero-point level of the rocking mode (with a calculated harmonic frequency of 81 cm^{-1}) should occur below the barrier, giving rise to an SIHB motif for the front-side isomer. On the other hand, $CH_3CO_2^-\cdot H_2O$ (Figure 5, center panel) presents the intermediate case of a shallow BO curve which is noticeably flattened, but still displays a single minimum upon inclusion of the OH stretch zero-point energies (U_0^{ad}). This situation would give rise to very large amplitude zero-point motion along the rocking coordinate.

Two vibrationally excited adiabatic potential surfaces are important in the mid-IR, each denoted U_1^{ad}, and defined by $n_i = 1$ and $n_j = 0$ in eq 2. Note that in the acetate monohydrate, one of these (U_1^{ad}) develops a strong double minimum. Thus, in the case where the DIHB configuration of a monohydrate is only slightly lower in energy than the asymmetric SIHB form (i.e., a shallow BO potential), excitation of the symmetric OH stretching vibration should generically induce a *structural* change which favors the asymmetric form. Furthermore, because such a complex is characterized by very large zero-point motion along the water rock coordinate, we may expect excitation of the first vibrational state of the OH stretch to be accompanied by unusually strong activity involving this soft mode. Such an effect would be more pronounced in the OH region than in the lower energy OD range, as is observed to be the case. It would be valuable to undertake a more sophisticated theoretical treatment of such mode coupling to determine if this indeed lies at the heart of the observed complexity.

IV. Summary

We present mid-IR predissociation spectra of a series of molecular anion monohydrates in which the water molecule attaches to a triatomic binding site. With a third-row atom (S) in the triatomic motif, the water molecule forms two H bonds to the ion and displays a very simple OH stretching spectrum. Much more complicated spectra are observed in the $CH_3NO_2^-\cdot H_2O$ and $CH_3CO_2^-\cdot H_2O$ complexes, however, where a closer separation exists between the terminal oxygen atoms in the binding site than that displayed in the sulfur containing anions. The spectrum of $NO_2^-\cdot H_2O$, which involves the shortest binding domain of the anions in this report, yields the simple red-shifted spectrum expected for an asymmetric complex. Calculations indicate that the methylated complexes have very shallow potentials for the water molecule rocking motion and that the OH stretching frequencies are dramatically changing along this coordinate. This vibrationally induced structure change provides a possible explanation for the complexity of these spectra in the OH stretching region, in contrast to the much simpler spectra in the OD region for the $CH_3NO_2^-\cdot D_2O$ and $CH_3NO_2^-\cdot HDO$ complexes.

Acknowledgment. We thank the National Science Foundation, Experimental Physical Chemistry Division for support of this work. We also acknowledge Prof. K. D. Jordan for valuable discussions on the ab initio structures of the $CH_3NO_2^-$ and $CH_3CO_2^-$ monohydrate complexes.

References and Notes

(1) Ayotte, P.; Weddle, G. H.; Kim, J.; Johnson, M. A. *J. Am. Chem. Soc.* **1998**, *120*, 12361.

(2) Ayotte, P.; Kelley, J. A.; Nielsen, S. B.; Johnson, M. A. *Chem. Phys. Lett.* **2000**, *316*, 455.

(3) Johnson, M. S.; Kuwata, K. T.; Wong, C.-K.; Okumura, M. *Chem. Phys. Lett.* **1996**, *260*, 551.

(4) Marcus, Y.; *Ion Solvation*; Wiley-Interscience: Chichester, U.K., 1985.

(5) Zhan, C.-G.; Iwata, S. *Chem. Phys. Lett.* **1995**, *232*, 72.

(6) Bentley, J.; Collins, J. Y.; Chipman, D. M. *J. Phys. Chem. A* **2000**, *104*, 4629.

(7) Surber, E.; Anathavel, S. P.; Sanov, A. *J. Chem. Phys.* **2002**, *116*, 1920.

(8) Woronowicz, E. A.; Robertson, W. H.; Weddle, G. H.; Johnson, M. A.; Myshakin, E. M.; Jordan, K. D. *J. Phys. Chem. A* **2002**, *106*, 7086.

(9) Weber, J. M.; Kelley, J. A.; Nielsen, S. B.; Ayotte, P.; Johnson, M. A. *Science* **2000**, *287*, 2461.

(10) Robertson, W. H.; Johnson, M. A.; Myshakin, E. M.; Jordan, K. D. *J. Phys. Chem. A* **2002**, *106*, 10010.

(11) Orden, A. V.; Saykally, R. J. *Chem. Rev.* **1998**, *98*, 2313.

(12) Ayotte, P.; Weddle, G. H.; Kim, J.; Johnson, M. A. *Chem. Phys.* **1998**, *239*, 485.

(13) Klots, C. E. *J. Chem. Phys.* **1985**, *83*, 5854.

(14) Okumura, M.; Yeh, L. I.; Myers, J. D.; Lee, Y. T. *J. Chem. Phys.* **1986**, *85*, 2328.

(15) Okumura, M.; Yeh, L. I.; Myers, J. D.; Lee, Y. T. *J. Phys. Chem.* **1990**, *94*, 3416.

(16) Kelley, J. A.; Weber, J. M.; Lisle, K. M.; Robertson, W. H.; Ayotte, P.; Johnson, M. A. *Chem. Phys. Lett.* **2000**, *327*, 1.

(17) Corcelli, S. A.; Kelley, J. A.; Tully, J. C.; Johnson, M. A. *J. Phys. Chem. A* **2002**, *106*, 4872.

(18) Nielsen, S. B.; Ayotte, P.; Kelley, J. A.; Johnson, M. A. *J. Chem. Phys.* **1999**, *111*, 9593.

(19) Robertson, W. H.; Kelley, J. A.; Johnson, M. A. *Rev. Sci. Instrum.* **2000**, *71*, 4431.

(20) Johnson, M. A.; Lineberger, W. C.; in *Techniques for the study of Gas-Phase Ion Molecule Reactions*: Farrar, J. M., Saunders, W., Eds; Wiley: New York, 1988; p 591.

(21) Frisch, M. J.; Trucks, G. W.; Schlegel, H. B.; Scuseria, G. E.; Robb, M. A.; Cheeseman, J. R.; Zakrzewski, V. G.; Montgomery, J. A., Jr.; Stratmann, R. E.; Burant, J. C.; Dapprich, S.; Millam, J. M.; Daniels, A. D.; Kudin, K. N.; Strain, M. C.; Farkas, O.; Tomasi, J.; Barone, V.; Cossi, M.; Cammi, R.; Mennucci, B.; Pomelli, C.; Adamo, C.; Clifford, S.; Ochterski, J.; Petersson, G. A.; Ayala, P. Y.; Cui, Q.; Morokuma, K.; Malick, D. K.; Rabuck, A. D.; Raghavachari, K.; Foresman, J. B.; Cioslowski, J.; Ortiz, J. V.; Baboul, A. G.; Stefanov, B. B.; Liu, G.; Liashenko, A.; Piskorz, P.; Komaromi, I.; Gomperts, R.; Martin, R. L.; Fox, D. J.; Keith, T.; Al-Laham, M. A.; Peng, C. Y.; Nanayakkara, A.; Gonzalez, C.; Challacombe, M.; Gill, P. M. W.; Johnson, B.; Chen, W.; Wong, M. W.; Andres, J. L.; Head-Gordon, M.; Replogle, E. S.; Pople, J. A. *Gaussian 98*; Gaussian, Inc.: Pittsburgh, PA, 1998.

(22) Robertson, W. H.; Weddle, G. H.; Kelley, J. A.; Johnson, M. A. *J. Phys. Chem. A* **2002**, *106*, 1205.

(23) Weber, J. M.; Robertson, W. H.; Johnson, M. A. *J. Chem. Phys.* **2001**, *115*, 10718.

(24) Thompson, W. H.; Hynes, J. T. *J. Am. Chem. Soc.* **2000**, *122*, 6278.

(25) Rice, B. M.; Pai, S. V.; Chabalowski, C. F. *J. Phys. Chem. A* **1998**, *102*, 6950.

(26) Surber, E.; Sanov, A. *J. Chem. Phys.* **2002**, *116*, 5921.

(27) McKee, M. L.; Wine, P. H. *J. Am. Chem. Soc.* **2001**, *123*, 2344.

(28) Goumri, A.; Rocha, J. R.; Laakso, D.; Smith, C. E.; Marshall, P. *J. Phys. Chem. A* **1999**, *103*, 11328.

(29) Polasek, M.; Turecek, F. *J. Phys. Chem. A* **1999**, *103*, 9241.

(30) Compton, R. N.; Carman, H. S., Jr.; Desfracois, C.; Abdoul-Carime, H.; Schermann, J. P.; Hendricks, J. H.; Lyapustina, S. A.; Bowen, K. H. *J. Chem. Phys.* **1996**, *105*, 3472.

(31) *NIST Chemistry WebBook*; National Institute of Standards and Technology: Gaithersburg, MD, 2001.

(32) Cumming, J. B.; Kebarle, P. *Can. J. Chem.* **1978**, *56*, 1.

(33) Staib, A.; Hynes, J. T. *Chem. Phys. Lett.* **1993**, *204*, 197.

(34) Gutsev, G. L.; Bartlett, R. J. *J. Chem. Phys.* **1996**, *105*, 8785.

(35) Wilmshurst, J. K. *J. Chem. Phys.* **1956**, *25*, 1171.

(36) Barnes, A. J.; Hallam, H. E. *T. Faraday Soc.* **1970**, *66*, 1920.

(37) Yates, B. F.; Schaefer, H. F., III.; Lee, T. J.; Rice, J. E. *J. Am. Chem. Soc.* **1988**, *110*, 6327.

(38) Weber, J. M.; Kelley, J. A.; Robertson, W. H.; Johnson, M. A. *J. Chem. Phys.* **2001**, *114*, 2698.